AGU PUBLICATIONS

Paleoceanography

RESEARCH ARTICLE
10.1002/2016PA002956

Key Points:
- Six ice sheet meltwater events identified in Gulf of Mexico seawater $\delta^{18}O$ record from 2.55-1.70 Ma
- Events are typically long, occur late in benthic $\delta^{18}O$ deglaciations, and line up with summer insolation
- This challenges view of early Pleistocene marine $\delta^{18}O$ as simply recording obliquity-driven Northern Hemisphere ice volume

Supporting Information:
- Supporting Information S1
- Supporting Information S2

Correspondence to:
J. D. Shakun,
jeremy.shakun@bc.edu

Citation:
Shakun, J. D., M. E. Raymo, and D. W. Lea (2016), An early Pleistocene Mg/Ca-$\delta^{18}O$ record from the Gulf of Mexico: Evaluating ice sheet size and pacing in the 41-kyr world, *Paleoceanography*, *31*, 1011–1027, doi:10.1002/2016PA002956.

Received 25 MAR 2016
Accepted 5 JUL 2016
Accepted article online 11 JUL 2016
Published online 25 JUL 2016

An early Pleistocene Mg/Ca-$\delta^{18}O$ record from the Gulf of Mexico: Evaluating ice sheet size and pacing in the 41-kyr world

Jeremy D. Shakun[1], Maureen E. Raymo[2], and David W. Lea[3]

[1]Department of Earth and Environmental Sciences, Boston College, Chestnut Hill, MA, USA, [2]Lamont-Doherty Earth Observatory, Columbia University, Palisades, NY, USA, [3]Department of Earth Science, University of California, Santa Barbara, CA, USA

Abstract Early Pleistocene glacial cycles in marine $\delta^{18}O$ exhibit strong obliquity pacing, but there is a perplexing lack of precession variability despite its important influence on summer insolation intensity – the presumed forcing of ice sheet growth and decay according to the Milankovitch hypothesis. This puzzle has been explained in two ways: Northern Hemisphere ice sheets instead respond to insolation integrated over the summer, which is mostly controlled by obliquity, or anti-phased precession-driven variability in ice volume between the hemispheres cancels out in global $\delta^{18}O$, leaving the in-phase obliquity signal to dominate. We evaluated these ideas by reconstructing Laurentide Ice Sheet (LIS) meltwater discharge to the Gulf of Mexico from 2.55-1.70 Ma using foraminiferal Mg/Ca and $\delta^{18}O$. Our $\delta^{18}O_{sw}$ record displays six prominent anomalies, which likely reflect meltwater pulses, and they have several remarkable characteristics: (1) their presence suggests that the LIS expanded into the mid-latitudes numerous times; (2) they tend to occur or extend into interglacials in benthic $\delta^{18}O$; (3) they generally correlate with summer insolation intensity better than integrated insolation forcing; and (4) they are perhaps smaller in amplitude but longer in duration than their late Pleistocene counterparts, suggesting comparable total meltwater fluxes. Overall, these observations suggest that the LIS was large, sensitive to precession, and decoupled from marine $\delta^{18}O$ numerous times during the early Pleistocene – observations difficult to reconcile with a straightforward interpretation of the early Pleistocene marine $\delta^{18}O$ record as a proxy for Northern Hemisphere ice sheet size driven by obliquity forcing at high latitudes.

1. Introduction

The Milankovitch hypothesis holds that ice sheets are sensitive to the intensity of summer insolation, which depends on both the tilt of the earth – which varies with the 41-kyr obliquity cycle – and the seasonal distance to the sun – which varies with the 23-kyr precession cycle. The Milankovitch model has had considerable success in explaining late Pleistocene ice volume variations of the past one million years, cycles that are concentrated at eccentricity, precession and obliquity frequencies as well as their multiples [*Huybers*, 2011; *Imbrie and Imbrie*, 1980; *Raymo*, 1997]. Nonetheless, the marine $\delta^{18}O$ record suggests that the immediately preceding glacial cycles of the late Pliocene-early Pleistocene (3–1 Ma) occurred at the almost purely 41-kyr pacing (Figure 1b) [*Huybers*, 2007; *Pisias and Moore*, 1981; *Raymo and Nisancioglu*, 2003; *Ruddiman et al.*, 1989]. This 41-kyr world is difficult to reconcile with the Milankovitch hypothesis – why is precession variability absent in the early Pleistocene if summer insolation intensity controls ice sheet mass balance?

Two hypotheses have been suggested to rectify the apparent conflict between the ice volume changes predicted by Milankovitch forcing and those actually observed in the marine $\delta^{18}O$ record. The Integrated Insolation hypothesis points out that the most intense summers are also the shortest, since the Earth orbits faster when closer to the sun [*Huybers*, 2006]. Since these competing precession-driven effects, intensity versus duration, nearly cancel out when integrated over the course of the summer, one might not expect to see a strong precession signal in ice volume variability. The Antiphase hypothesis instead argues that ice sheets are driven by both obliquity and precession (as expressed in summer insolation intensity), but while obliquity is in phase between the hemispheres (i.e., increased axial tilt causes stronger summers in both hemispheres), precession forcing is anti-phased (i.e., when one hemisphere's summer occurs closest to the sun, the other's summer occurs farthest from the sun six months later) [*Raymo et al.*, 2006]. Therefore, if a record of global ice volume, such as marine $\delta^{18}O$ or sea level, was recording ice volume changes in both hemispheres, it would

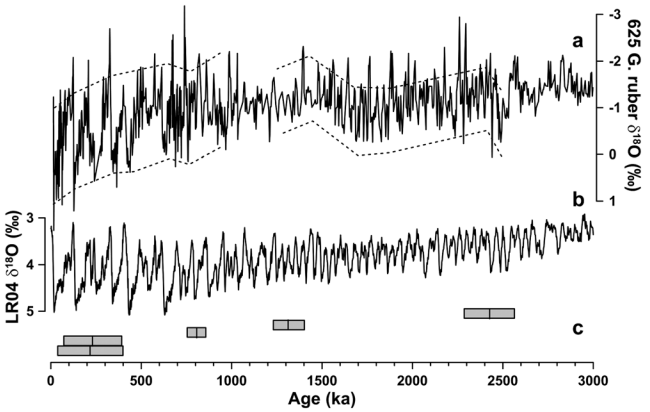

Figure 1. Ocean and land records of Pleistocene ice sheets. (a) *G. ruber* $\delta^{18}O$ from Site 625 in the Gulf of Mexico [*Joyce et al.*, 1990]. *Joyce et al.* [1993] interpreted negative excursions beyond the range they considered attributable to global glacial-interglacial cycles (dashed lines; 1.3‰ in the early Pleistocene, 2‰ in the late Pleistocene) to reflect input of isotopically depleted Laurentide meltwater via the Mississippi River. (b) The LR04 benthic $\delta^{18}O$ stack [*Lisiecki and Raymo*, 2005]. (c) ^{26}Al-^{10}Be ages of Laurentide Ice Sheet tills in Missouri at 39°N [*Balco and Rovey*, 2010].

only capture the in-phase behavior at the 41-kyr obliquity period, while antiphased precession variability would largely cancel out. The key to distinguishing between these hypotheses is a reconstruction that isolates Laurentide Ice Sheet (LIS) variability independent of, but co-registered with, the marine $\delta^{18}O$ record, to determine if ice sheet ablation was driven by obliquity alone or both obliquity and precession. Here we present records of southern LIS meltwater to the Gulf of Mexico (GOM) based on planktic foraminiferal Mg/Ca-$\delta^{18}O$ and benthic $\delta^{18}O$ at Ocean Drilling Program (ODP) Site 625 from 2.55-1.70 Ma, an interval that features prominent 41-kyr glacial cycles in the global benthic LR04 stack [*Lisiecki and Raymo*, 2005].

2. Background

Nearly every numerical ice sheet model that has been used to study the Plio-Pleistocene predicts strong precession-driven ice volume variability, in keeping with the Milankovitch hypothesis [*Abe-Ouchi et al.*, 2013; *Berger et al.*, 1999; *Clark and Pollard*, 1998; *Nisancioglu*, 2004]. A notable exception is the work of *Huybers and Tziperman* [2008], who were able to simulate 41-kyr glacial cycles if two conditions were met: the ablation zone was north of ~60°N, where obliquity forcing dominates, and the ablation season was long enough for summer duration to offset summer intensity. Unfortunately, the typical size of the early Pleistocene ice sheets is rather unclear from the geologic record. Taken at face value, the marine $\delta^{18}O$ record suggests that early Pleistocene ice sheets were less voluminous than their late Pleistocene counterparts [*Lisiecki and Raymo*, 2005]; however, mid-continent tills as far south as Kansas and Missouri indicate that the Laurentide Ice Sheet (LIS) reached a maximum extent at that time comparable to that observed in the late Pleistocene (Figure 1c, 2) [*Balco and Rovey*, 2010; *Roy et al.*, 2004].

The Regolith Hypothesis of *Clark and Pollard* [1998] reconciles these two observations by invoking extensive early Pleistocene ice sheets with a low profile geometry, which resulted from rapid ice flow over a thick bed of deformable regolith. They further propose that this thick regolith bed slowly eroded away, eventually resulting in ice sheets that were more sluggish, thicker, and less responsive to insolation forcing, leading to the longer period variability observed in the late Pleistocene. Alternatively, the Antiphase hypothesis can accommodate larger ice sheets whose full signal is not recorded in proxies such as $\delta^{18}O$ that integrate an out-of-phase signal from both poles. Ultimately, the physical evidence for large ice sheets, upon which the Regolith Hypothesis is predicated, consists of perhaps only two tills, and the interpretation of this evidence remains controversial (Figure 1c) [*Balco and Rovey*, 2010; *Roy et al.*, 2004].

It is thus unclear if the LIS routinely advanced as far south as the central United States during the early Pleistocene and responded to the precession forcing that would dominate at these latitudes. If so, this pattern would strengthen the Regolith and the Antiphase Hypotheses [*Raymo et al.*, 2006], and open up the possibility that the early Pleistocene ice sheets were as voluminous as their late Pleistocene counterparts, but masked in the global $\delta^{18}O$ record by hemispherically antiphased precession variability. If, on the other hand, the LIS rarely advanced into the contiguous US and responded only to high latitude obliquity, these two hypotheses would be commensurately weakened and a more straightforward interpretation of the $\delta^{18}O$ record, in line with the Integrated Insolation hypothesis, would be implied [*Huybers*, 2006]. What is needed to address these issues is an early Pleistocene record of variability of the southern margin of the LIS.

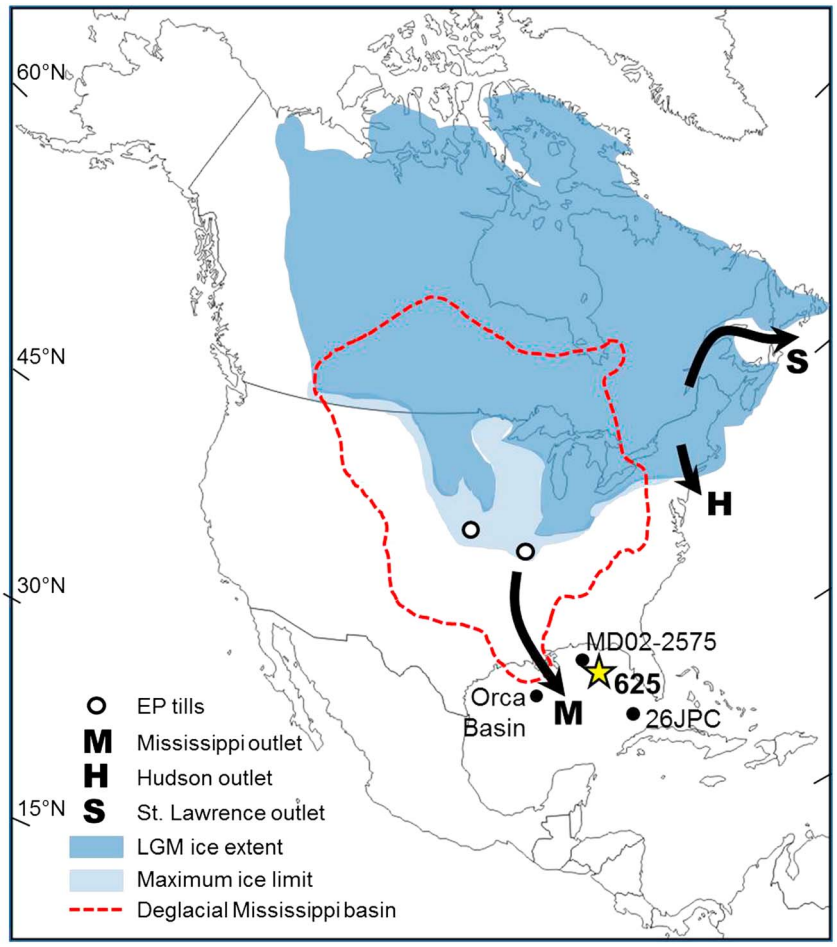

Figure 2. Map of North America showing Laurentide Ice Sheet extent during the Last Glacial Maximum (dark blue) and at its Pleistocene maximum (light blue), as well as the modeled Mississippi cryohydrological basin midway through the last deglaciation (red dashed line, 14.5 ka basin extent from ICE-5G/VM2 model [*Wickert et al.*, 2013]). Locations of ODP Site 625 and other Gulf of Mexico cores discussed in the text (black dots; Orca Basin, [*Flowers et al.*, 2004]; MD02-2575, [*Ziegler et al.*, 2008], 26JPC [*Schmidt and Lynch-Stieglitz*, 2011]), and early Pleistocene tills near the Laurentide maximum southern limit, two in the eastern area that have been burial dated with cosmogenic nuclides to 2.42 ± 0.14 and 1.31 ± 0.09 Ma and one in the western area that pre-dates a 2.0 Ma Yellowstone tephra (white dots, though note that the tills have been identified at multiple sites in each area; [*Balco and Rovey*, 2010; *Roy et al.*, 2004]). Arrows show the major drainage pathways for southern Laurentide Ice Sheet runoff.

Joyce et al. [1990, 1993] generated a Plio-Pleistocene planktonic $\delta^{18}O$ record from Site 625 near the mouth of the Mississippi River in the GOM, loosely dated by tuning the 41-kyr component to obliquity. Their record shows a number of large (≥2‰) negative $\delta^{18}O$ isotope anomalies beginning at ~2.3 Ma, which Joyce et al. attributed to meltwater events from the southern LIS (Figure 1a). This conclusion was based on the anomalies' magnitude, absence in deeper-dwelling foraminifera, and difficulty of being explained by temperature or fluvial-pluvial events. The *Joyce et al.* [1990, 1993] $\delta^{18}O$ record therefore provides a potential way to evaluate the above hypotheses, but it currently lacks (1) verification of its extreme isotope anomalies, (2) a benthic chronology to enable an assessment of the phasing of LIS melt relative to precession and obliquity, and (3) a sea surface temperature (SST) record to isolate the seawater $\delta^{18}O$ component of planktonic $\delta^{18}O$ ($\delta^{18}O_{sw}$). This last step is essential as precession-driven SST variability – a reasonable possibility in the GOM [*Ziegler et al.*, 2008] – would confound any attempt to determine whether the LIS exhibited precession variability using the existing planktic $\delta^{18}O$ record alone. We address each of these issues at Site 625.

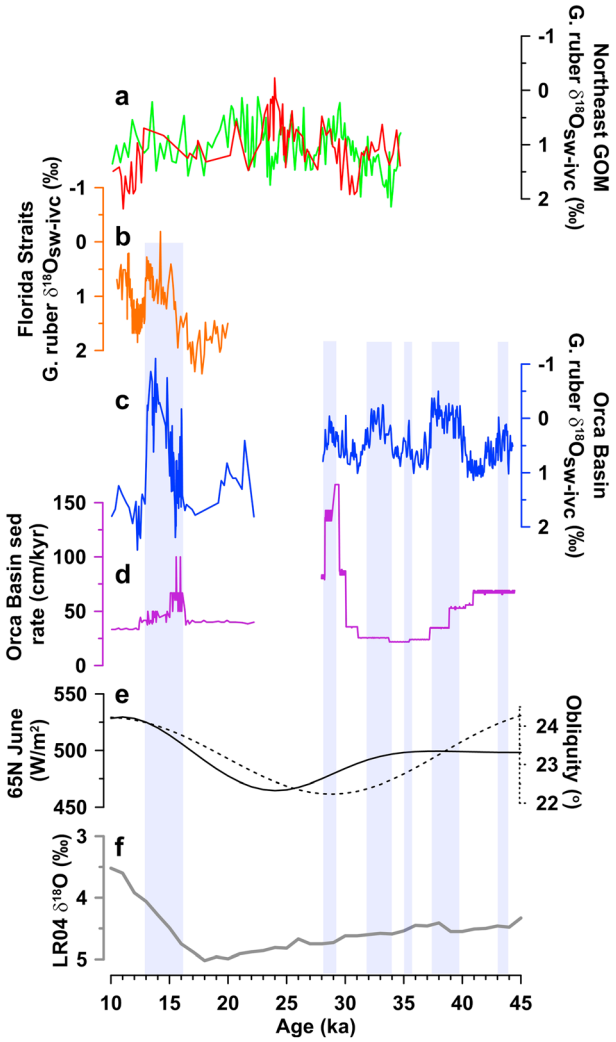

Figure 3. Gulf of Mexico $\delta^{18}O_{sw\text{-}ivc}$ records from the last glacial period. (a) *G. ruber* $\delta^{18}O_{sw\text{-}ivc}$ from Site 625 (red) [*Whitaker*, 2008] and MD02-2575 (green) [*Ziegler et al.*, 2008], both in the northeastern Gulf of Mexico. (**b**) *G. ruber* $\delta^{18}O_{sw\text{-}ivc}$ from 26JPC in the Florida Straits (orange) [*Schmidt and Lynch-Stieglitz*, 2011]. (c) *G. ruber* $\delta^{18}O_{sw\text{-}ivc}$ from the Orca Basin in the north-central Gulf of Mexico (blue) [*Flower et al.*, 2004; *Hill et al.*, 2006]. (d) Sedimentation rates in the Orca Basin (purple). (e) Boreal summer insolation and orbital obliquity [*Laskar et al.*, 2004]. (f) The LR04 benthic $\delta^{18}O$ stack [*Lisiecki and Raymo*, 2005]. Vertical blue bars highlight negative isotope excursions in the Orca Basin and Florida Straits interpreted as Laurentide Ice Sheet meltwater events; note that these isotopic features are weak or absent in the records from the northeastern Gulf of Mexico in panel a (though these records are relatively low resolution and weakly dated).

3. Core Setting and Last Glacial Context

Site 625 (28.83°N, 87.16°W, 889 m) is located in the northeast GOM along De Soto Canyon, 200 km east of the mouth of the Mississippi River, the major outlet for the southern LIS when it extends over the Great Lakes and blocks eastward drainage through the St. Lawrence and Hudson Rivers (Figure 2). During winter, cold fronts migrating off the continent drive vertical mixing of the top 200 m of the water column and SSTs reach a minimum of 19.7 °C. In the summer, the Loop Current fills the region with Caribbean waters that peak at 29.7 °C in association with a northward expansion of the Atlantic Warm Pool [*Ziegler et al.*, 2008]. Salinity near this site varies from 32.8 practical salinity units (psu) in summer to 35.8 psu in winter [*Antonov et al.*, 2010].

Planktonic $\delta^{18}O$ records from the western GOM and Florida Straits show clear signals of meltwater during the last deglaciation [*Aharon*, 2006; *Flower et al.*, 2004; *Kennett and Shackleton*, 1975; *Schmidt and Lynch-Stieglitz*, 2011]. The meltwater signal is especially well resolved in the anoxic Orca Basin, which displays an interval of pronounced $\delta^{18}O_{sw\text{-}ivc}$ (ice volume-corrected seawater $\delta^{18}O$) depletion from ~17-13 ka associated with initial retreat of the LIS northward across the Mississippi River basin (Figure 3c). This isotopic spike reaches nearly 3‰ in magnitude before abruptly returning to background values at the start of the Younger Dryas as meltwater was routed eastward through the St. Lawrence River [*Wickert et al.*, 2013]. This event coincides with the first half of the global deglaciation as recorded by the LR04 benthic stack [*Lisiecki and Raymo*, 2005], and slightly precedes peak forcing from obliquity and boreal summer insolation intensity, which are nearly in phase with each other across the last deglaciation (Figure 3e,f). The Orca Basin $\delta^{18}O_{sw\text{-}ivc}$ record also suggests earlier episodes of meltwater input to the GOM as the LIS expanded into and presumably oscillated in the upper Mississippi basin during the last glacial period, though these are smaller in magnitude (1‰) and shorter in duration (1–3 kyr) (Figure 3c) [*Hill et al.*, 2006]. Importantly, however, the deglacial meltwater signal seems to be absent in $\delta^{18}O$ records from the northeastern GOM [*Ziegler et al.*, 2008], including Site 625 [*Whitaker*, 2008], highlighting the spatial complexity of meltwater plumes

(Figure 3a). That said, these two records are relatively low resolution and weakly dated over the last deglaciation, admitting the possibility that meltwater was present in the northeastern GOM, but simply missed by these records.

4. Materials and Methods

4.1. Sediment Processing

The original *Joyce et al.* [1990, 1993] samples could not be located. We consequently obtained new samples from 89.68-119.93 meters below sea floor (mbsf) in 625 from the ODP Gulf Coast Repository, with an average sample spacing of 7 cm. Samples were 2 cm thick and ~15 cc in volume. After freeze drying, samples were disaggregated through agitation in a sodium hexametaphosphate solution, washed through a 63 μm sieve with deionized water, and oven-dried at 40 °C. Foraminifera were picked by hand using a binocular microscope.

4.2. Benthic Stable Isotopes

Costanza [2007] generated a ~15 cm-resolution $\delta^{18}O$ record at Site 625 over the depths of interest on mixed *Cibicidoides* species (>250 μm). He found no evidence for species isotopic offsets. We doubled the resolution to ~7 cm over the interval 89.68-109.3 mbsf also using mixed *Cibicidoides* species (>150 μm), and spliced our data with *Costanza*'s [2007]. An average of six individuals (range of 1 to 22) were used per sample; the tests were crushed, homogenized, and a split was removed for measurement. *Costanza*'s [2007] samples were analyzed at the University of California-Santa Cruz on a Micromass Prism III isotope ratio mass spectrometer (IRMS), and our samples were measured on a Finnigan MAT 252 IRMS at Oregon State University from 89.68-100.72 mbsf and an Elementar Isoprime 100 at Lamont-Doherty Earth Observatory for 100.82-109.3 mbsf. Typical 1σ measurement uncertainties are 0.06 ‰ for $\delta^{18}O$ and 0.02 ‰ for $\delta^{13}C$.

4.3. Age Model

The age model was developed by correlating the 625 benthic $\delta^{18}O$ record to the LR04 stack [*Lisiecki and Raymo*, 2005]. Paleomagnetic data below the Brunhes/Matuyama boundary (780 ka) at 59 mbsf are not useful at Site 625 due to weak remnant magnetism [*Clement*, 1985], but several biostratigraphic datums help to broadly place the record in time, and 35 $\delta^{18}O$ tie points were then used to more precisely anchor it to the LR04 stack (Figure 4). Tie points are given in the Supplementary data.

4.4. Planktic Stable Isotopes

We measured stable isotopes on 344 *G. ruber* white (sensu stricto, s.s.) (250–355 μm) samples using 5–50 individuals per sample. Measurements were performed at the University of California-Santa Barbara on a GV Instruments Isoprime IRMS following the protocol of *Lalicata and Lea* [2011], at Lamont-Doherty Earth Observatory on an Elementar Isoprime 100, and at Oregon State University on a Finnigan MAT 252 IRMS. Typical 1σ analytical uncertainties are 0.06 ‰ for $\delta^{18}O$ and 0.02 ‰ for $\delta^{13}C$. All data, including which lab samples were analyzed in, are given in the Supplementary data.

4.5. Planktic Trace Metals

We analyzed trace metals on 779 *G. ruber* white (s.s.) (250–355 μm) samples, including 145 replicates. Typically ~45 individuals were used per sample, or ~80 individuals for replicates. Samples were cleaned at UC-Santa Barbara following the protocol of *Lea et al.* [2000] and *Martin and Lea* [2002] and at Lamont-Doherty Earth Observatory following the protocol outlined in *Arbuszewski et al.* [2010], both with repeated MilliQ/methanol rinses to remove clays and full reductive and oxidative steps. Samples were measured by either inductively coupled plasma mass spectrometry at UC-Santa Barbara or inductively coupled plasma optical emission spectrometry at Lamont-Doherty Earth Observatory. A comparison between the trace metal data from the two labs is shown in Figure S3. Replicates were only run within, and not between, labs. The pooled standard deviation of Mg/Ca replicates, which reflects both analytical precision and sample heterogeneity, averaged 4.9%, equivalent to ~0.5 °C. For comparison, *G. ruber* replicates from tropical Pacific cores had pooled standard deviations of 2-3% [*Lea et al.*, 2000], suggesting that sample heterogeneities are greater at Site 625, with enhanced seasonality, millennial-scale variability, or diagenetic overprinting as potential causes.

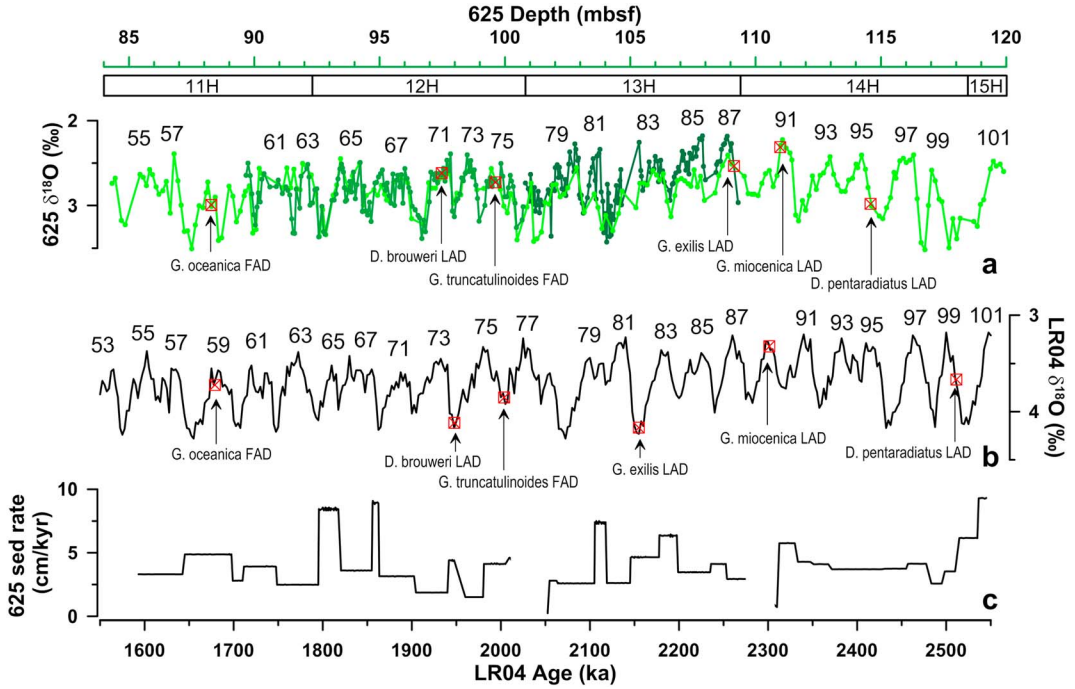

Figure 4. Correlation of the (a) 625 benthic $\delta^{18}O$ record on its depth scale (top x-axis) to the (b) LR04 stack and time scale (bottom x-axis) [*Lisiecki and Raymo*, 2005], (c) with implied sedimentation rates. Numbers above each isotope record refer to marine isotope stages. Core sections are shown at the top. Biostratigraphic datums are represented by red symbols and labeled; depths of biostratigraphic events in 625 are from *Joyce et al.* [1990] and ages of the datums plotted on the LR04 stack are taken from *Berggren et al.* [1995]. 625 $\delta^{18}O$ data were analyzed at University of California-Santa Cruz (light green), Lamont-Doherty Earth Observatory (dark green), and Oregon State University (medium green).

To evaluate diagenetic overprinting, we analyzed Al/Ca, Fe/Ca, and Mn/Ca [*Barker et al.*, 2003; *Lea et al.*, 2005] in Site 625 samples (Figure S1). Mg/Ca exhibits significant correlations with Al/Ca, Fe/Ca, and Mn/Ca during brief intervals of the record (Figure S3), but overall correlations are not significant (Figure S2). Correlations between replicates of the same sample are weak for Al and Mn ($r^2 = 0.04$ and 0.03, $p = 0.03$ and 0.03) but significant for Fe ($r^2 = 0.15$, $p < 0.01$) (Figure S4), suggesting that Fe-Mg-rich diagenetic overprints might influence sample heterogeneity. In addition, the slope of the Mg-Fe relationship in replicates is 1.3, implying that a 0.3 mmol/mol anomaly in Fe/Ca could yield a ~1 °C bias on Mg/Ca. Nonetheless, there are only a few intervals with significant Fe-Mg correlation over the whole record (Figure S3h) and point-to-point variability in Fe/Ca is less than 0.1 mmol/mol over 90% of the data, suggesting that diagenetic influence on Mg/Ca is typically small compared to uncertainty in Mg/Ca and likely restricted to these intervals. We also performed flow-though analysis [*Klinkhammer et al.*, 2004] to ascertain if this approach could reveal potential contaminant patterns. The data [*Shakun and Klinkhammer*, unpublished, 2011], do not reveal clear contaminant patterns nor do they reveal clearer Mg/Ca oscillations than are present in the batch-run data. Dissolution is likely relatively unimportant given the shallow depth of the site (889 m).

4.6. $\delta^{18}O_{sw}$

SST was calculated using the planktic multi-species equation of *Dekens et al.* [2002] and *Anand et al.* [2003]: $Mg/Ca = 0.38*\exp(0.09*SST)$. $\delta^{18}O_{sw}$ was calculated as the residual of planktic $\delta^{18}O$ after removing the SST component using the equation: $\delta^{18}O_{sw} = 0.27 + (SST - 16.5 + 4.8*\delta^{18}O)$ [*Bemis et al.*, 1998]. We note that trace metals and stable isotopes were measured on splits of the same sample for only 87 samples; for all other samples, different individuals were used for Mg/Ca and $\delta^{18}O$. We also used the *Joyce et al.* [1990] $\delta^{18}O$ measurements for 84 of our Mg/Ca samples that did not have corresponding $\delta^{18}O$ values. In addition, we calculated $\delta^{18}O_{sw}$ from Mg/Ca and $\delta^{18}O$ samples that had at least 1 cm of overlap (all samples are 2 cm thick). This yielded a total of 384 $\delta^{18}O_{sw}$ values. Excluding the $\delta^{18}O_{sw}$ points derived from *Joyce et al.* [1990] $\delta^{18}O$ or offset Mg/Ca and $\delta^{18}O$ measurements does not eliminate any of the negative isotope excursions interpreted as

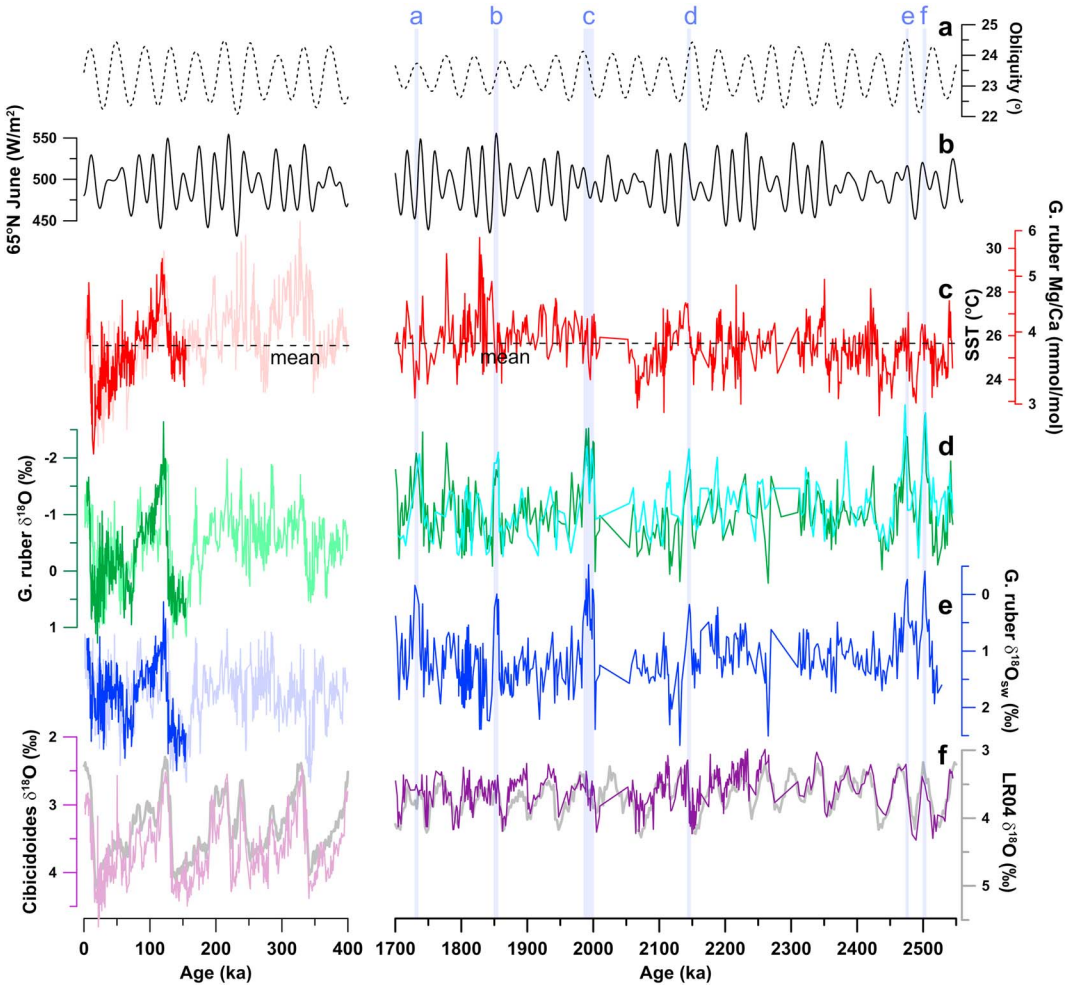

Figure 5. Orbital forcing and northeastern Gulf of Mexico data for the late (left) and early (right) Pleistocene from Site 625 (dark colors) and MD02-2575 (light colors). (a) Obliquity [*Laskar et al.*, 2004]. (b) 65°N June insolation [*Laskar et al.*, 2004]. (c) *G. ruber* Mg/Ca SSTs (red), with early and late Pleistocene mean values denoted (dashed lines). (d) *G. ruber* $\delta^{18}O$ (green). The original 625 *G. ruber* $\delta^{18}O$ record from *Joyce et al.* [1990] is also shown in light blue on our new age model. (e) *G. ruber* $\delta^{18}O_{sw}$ (i.e., SST-corrected $\delta^{18}O$) (blue) (f) Benthic $\delta^{18}O$ (purple) and the LR04 stack (gray; [*Lisiecki and Raymo*, 2005]). Negative $\delta^{18}O_{sw}$ anomalies interpreted as meltwater events are highlighted by the vertical blue bands and labeled a-f. Early Pleistocene data are from our study at Hole 625B, 0–150 ka data are from *Whitaker* [2008] at Hole 625C, and 0–400 ka data are from *Ziegler et al.* [2008] at MD02-2575.

meltwater events below, but it could reduce the peak magnitude or duration of some (Figure S5). Following *Lea et al.* [2000], we estimate errors of at least ±0.2 ‰ on $\delta^{18}O_{sw}$, and emphasize that errors will be higher for samples that did not have Mg/Ca and $\delta^{18}O$ measured on splits of the same carbonate.

5. Results

The age model indicates that our record spans 1695–2545 ka (Marine Isotope Stage (MIS) 59 to 101; Figure 4), ranging from 100 to 200 kyr older than the planktic-based chronology estimated by *Joyce et al.* [1993]. Sedimentation rates average 4 cm kyr^{-1} and vary within approximately a factor of two (Figure 4c). The benthic $\delta^{18}O$ correlation to the LR04 stack is clear for the lower half of the record. MIS 77 and 89 are not evident in the $\delta^{18}O$ record and from their likely correlations with core breaks, we infer that they were lost during coring (this interval was single-cored). $\delta^{18}O$ ties to LR04 are more ambiguous for the upper half of the record, perhaps due to missing core segments, noisy $\delta^{18}O$ data related to local hydrologic or temperature variability, or slight inter-species differences. Ages of biostratigraphic datums in 625 on our age model are broadly similar to those assigned by the astro-magneto-radiochronology of *Berggren et al.* [1995], with offsets ranging

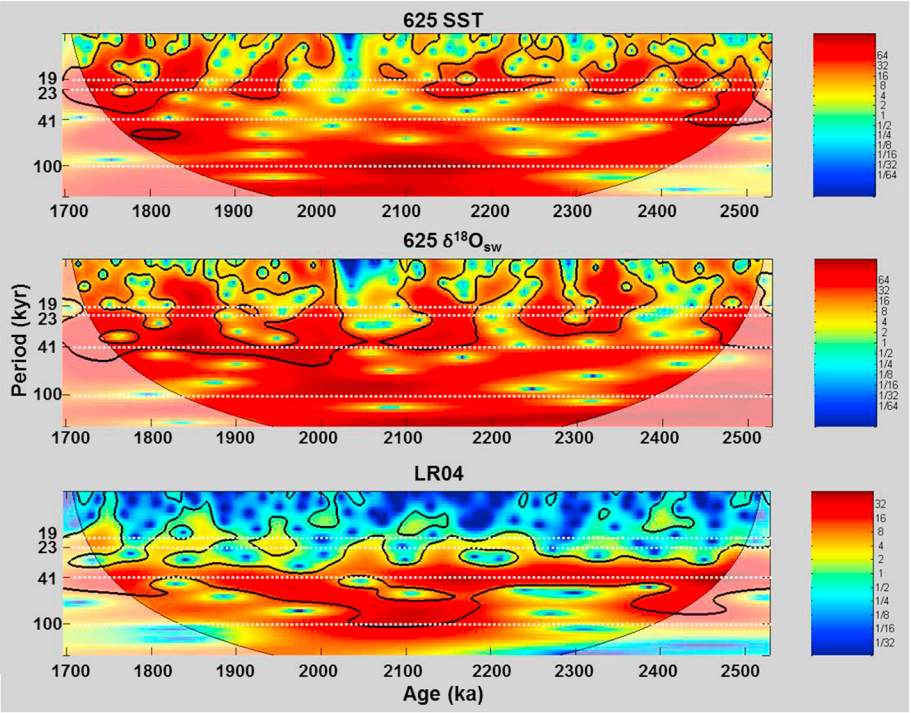

Figure 6. Wavelet spectra for 625 Mg/Ca SST (top), 625 $\delta^{18}O_{sw}$ (middle), and the LR04 stack (bottom) [*Lisiecki and Raymo*, 2005].

from 120 kyr older to 82 kyr younger. Such differences could arise for a variety of reasons, including time transgressive datums associated with species migration [*Weaver and Raymo*, 1989], preferential dissolution, bioturbation, or downslope sediment reworking. In any case, we suggest based on the combined isotopic and biostratigraphic constraints that our age model is robust prior to 2050 ka, but could be in error by up to a couple of glacial cycles thereafter. Such offsets of course would not affect the relative timing of the 625 SST and $\delta^{18}O$ records. Moreover, since the 625 record is tied into the 41-kyr rhythm of the early Pleistocene through correlation to the LR04 stack, misidentification of cycles would also likely have modest effects on the orbital-scale power in wavelet spectra and the phasing relative to obliquity. Nonetheless, this ambiguity does introduce uncertainty into absolute ages and thus into the relationship between variables measured at 625 and elsewhere, and potentially also to the relationship with precession. Mean sampling resolution for the benthic $\delta^{18}O$, planktic $\delta^{18}O$, and Mg/Ca records are 1.9, 2.6, and 1.3 kyr, and the derived $\delta^{18}O_{sw}$ reconstruction has a 2.2 kyr average resolution.

Our *G. ruber* $\delta^{18}O$ record is quite similar to the one originally produced by *Joyce et al.* [1990] (Figure 5d). Most importantly, nearly all of the light isotope anomalies identified by *Joyce et al.* [1990] are replicated in our record, confirming that they are robust features. *Costanza* [2007] measured the $\delta^{18}O$ of 10 individual forams per sample in 10 samples across the anomaly at 2150 ka and found that while the average $\delta^{18}O$ at each depth tracked the *Joyce et al.* [1990] data, the range among individuals at a given depth was large (up to 3.5 ‰). This high intra-sample variability may help to explain some of the point-to-point differences between our record and *Joyce et al.* [1990].

The *G. ruber* Mg/Ca SST reconstruction exhibits 2–4 °C peak-to-peak glacial cycles that roughly parallel the benthic $\delta^{18}O$ record, with generally warmer SSTs during interglacials and cooler SSTs during glacials (Figure 5c,f). Nonetheless, considerably more precession variability is present in SST than in benthic $\delta^{18}O$ (Figure 6). Mg/Ca reconstructions covering the last three glacial cycles exist at nearby ODP 625C and MD02-2575 [*Whitaker*, 2008; *Ziegler et al.*, 2008] and allow a comparison between SST variability during the early and late Pleistocene. Interestingly, average Mg/Ca values are identical between the two time intervals, which would suggest that the northern GOM experienced no mean cooling over the Pleistocene, assuming invariant seawater Mg/Ca (Figure 5c). Late Pleistocene SST precession cycles are modulated by larger

amplitude 100-kyr glacial cycles, however. Therefore, both maximum and minimum Mg/Ca values are more extreme than during the early Pleistocene.

Removing the SST component from the *G. ruber* $\delta^{18}O$ record leaves it relatively unchanged (Figure 5d,e) ($r^2 = 0.82$ and slope = 0.92 between the calcite $\delta^{18}O$ and the calculated $\delta^{18}O_{sw}$ record), highlighting the dominance of seawater $\delta^{18}O$ in controlling planktic $\delta^{18}O$ at 625. A wavelet analysis shows a greater concentration of variability near the obliquity period in the $\delta^{18}O_{sw}$ record, likely associated with changes in mean ocean composition over 41-kyr glacial cycles (Figure 6). Of greatest note, the *Joyce et al.* [1990] negative isotope anomalies remain prominent in the SST-corrected $\delta^{18}O_{sw}$ record, indicating that they do not reflect temperature. These anomalies are also unlikely to reflect ocean salinity processes given their 1–2 ‰ size, which would equate to unrealistically large 5–10 psu salinity changes based on modern $\delta^{18}O_{sw}$-salinity relationships in this region [*LeGrande and Schmidt*, 2006; *Wagner and Slowey*, 2011]. Instead, we interpret the $\delta^{18}O_{sw}$ anomalies as signals of isotopically depleted meltwater input to the GOM through the nearby mouth of the Mississippi River. Furthermore, *Joyce et al.* [1993] measured $\delta^{18}O$ on the deeper-dwelling foraminifer *N. dutertrei* across three of these events and found that none showed large excursions, consistent with them being confined near the surface as freshwater lenses. While foraminiferal Ba/Ca is also sometimes used as a proxy of freshwater input [*Schmidt and Lynch-Stieglitz*, 2011], values measured in our record are too high to reflect seawater Ba, and instead likely reflect unspecific contamination (Figure S6).

6. Discussion

6.1. Stable Pleistocene Sea Surface Temperatures?

Taken at face value, the Mg/Ca record suggests no long-term cooling of the GOM over the Pleistocene, which contrasts strongly with cooling trends observed in numerous areas around the world, including equatorial and coastal upwelling zones of the tropics and subtropics [*Fedorov et al.*, 2013], mid and high latitudes [*Bintanja and van de Wal*, 2008; *Fedorov et al.*, 2013], and perhaps the deep ocean [*Lisiecki and Raymo*, 2005; *Sosdian and Rosenthal*, 2009]. This lack of cooling may also be difficult to reconcile with the radiative forcing associated with a weakening greenhouse and expanding ice sheets over the Pleistocene [*Martinez-Boti et al.*, 2015], particularly given the proximity of Site 625 to the southern LIS.

Several possibilities may explain the stable GOM Mg/Ca values through the Pleistocene. On one hand, perhaps the GOM did not actually cool over this interval. A lack of early Pleistocene warmth in this region might be expected if, for instance, the LIS was already as extensive then as during the late Pleistocene [*Clark and Pollard*, 1998], or a stronger Atlantic Meridional Overturning Circulation offset global warmth here by exporting more heat from the low latitude Atlantic [*Bell et al.*, 2015]. On the other hand, the flat trend in GOM Mg/Ca could be a result of proxy bias. Indeed, other low latitude SST records with no long-term Pleistocene trends are also based on Mg/Ca (e.g., ODP sites 806, 999, 1143; [*O'Brien et al.*, 2014]), and disagree with cooling inferred from some organic proxies [*O'Brien et al.*, 2014; *Y. G. Zhang et al.*, 2014]. Moreover, both modeling and proxy data suggest that seawater Mg/Ca was lower during the early Pleistocene, which could artificially depress reconstructed SSTs [*Evans and Müller*, 2012; *Medina-Elizalde and Lea*, 2010; *Medina-Elizalde et al.*, 2008]. In addition, our early Pleistocene Mg/Ca record included a reductive cleaning step, whereas none of the late Pleistocene GOM Mg/Ca records discussed here did. Since selective dissolution during this step may reduce Mg/Ca by 10-15% [*Barker et al.*, 2003], our SST record could be artificially depressed relative to the late Pleistocene records. Correcting for this effect would shift early Pleistocene SSTs approximately 1–1.5 °C warmer.

Regardless of the reason for the long-term structure in GOM Mg/Ca from the early to late Pleistocene, both intervals display strong precession variability at shorter time scales. *Ziegler et al.* [2008] attribute this pattern over the past 300 kyr to summer insolation-driven shifts in the northward extension of the Atlantic Warm Pool, which currently expands to cover the GOM during summer, and its appearance in the early Pleistocene suggests that a similar mechanism may have operated then as well. Whereas late Pleistocene SSTs also exhibit considerable 100 kyr power, presumably related to ice sheet and/or greenhouse gas forcing, there is relatively little low frequency SST variability in the early Pleistocene (Figure 6).

6.2. Meltwater Events

We interpret six negative anomalies in the $\delta^{18}O_{sw}$ record as meltwater events (Figure 5e, 7c; Table 1). This may be a conservative estimate, but we only identified anomalies that are composed of multiple data points,

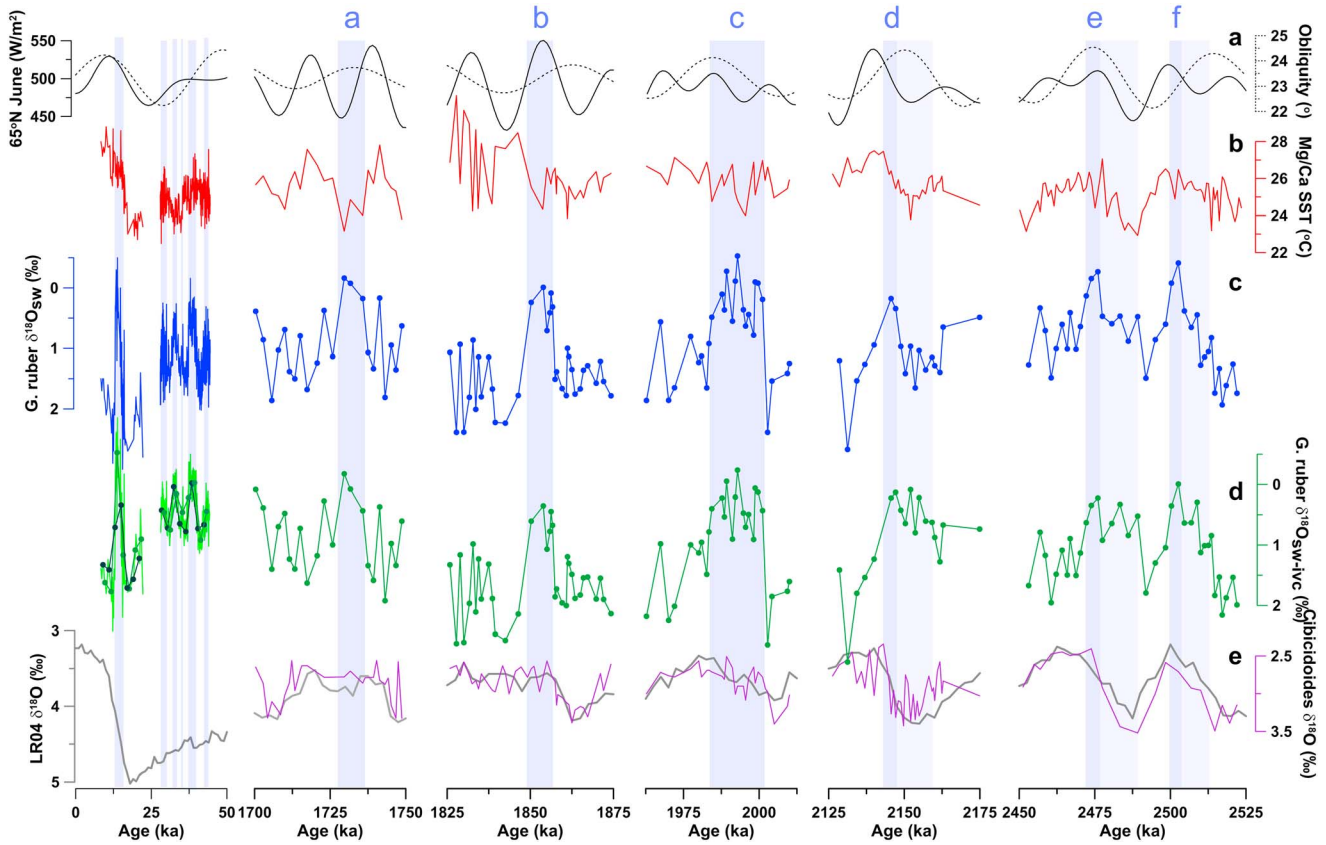

Figure 7. Gulf of Mexico meltwater events from the Orca Basin during the late Pleistocene (leftmost panel; [*Flower et al.*, 2004; *Hill et al.*, 2006]) and 625 for the early Pleistocene (five right panels; this study). (a) Orbital obliquity (dashed) and 65°N June insolation (solid) [*Laskar et al.*, 2004]. (b) *G. ruber* Mg/Ca SST. (c) *G. ruber* $\delta^{18}O_{sw}$. (d) *G. ruber* $\delta^{18}O_{sw\text{-}ivc}$, derived by subtracting a eustatic sea level reconstruction of ocean $\delta^{18}O$ [*Rohling et al.*, 2014] from the $\delta^{18}O_{sw}$ record. Leftmost panel shows Orca Basin data as originally published at high resolution (light green line) and after two iterations of resampling at the same resolution as the early Pleistocene 625 data (medium and dark green lines with datapoints). (e) 625 benthic $\delta^{18}O$ (purple) and the LR04 stack (gray; [*Lisiecki and Raymo*, 2005]). Vertical blue bars highlight $\delta^{18}O_{sw}$ anomalies interpreted as meltwater events; pale blue bars on events d-f highlight longer anomalies in $\delta^{18}O_{sw\text{-}ivc}$. Time is scaled identically in all panels.

are not present in the benthic $\delta^{18}O$ record, and are substantially larger than $\delta^{18}O_{sw}$ uncertainties as well as the range in marine $\delta^{18}O$ attributable to ice volume over early Pleistocene glacial cycles (≤0.5‰, [*Bintanja and van de Wal*, 2008]).

6.2.1. Phasing of Meltwater Events Relative to Marine $\delta^{18}O$ and Orbital Forcing

The meltwater events are distributed throughout the record, occurring near 1730, 1855, 1995, 2145, 2475, and 2500 ka, and we label them a-f (Table 1). While few in number, the timing of the meltwater events relative to benthic $\delta^{18}O$ provides a starting point to assess the phasing of southern LIS melt with respect to global glacial cycles during the early Pleistocene. Interestingly, this comparison shows that most of the meltwater

Table 1. Characteristics of the Early Pleistocene Gulf of Mexico $\delta^{18}O_{sw}$ Anomalies Interpreted as Meltwater Events

Meltwater event	Midpoint age (ka)	Duration (kyr)	Magnitude (‰)	Timing within glacial cycle	Summer insolation	Obliquity
a	1730	9	1.3	mid interglacial	decreasing	peak
b	1855	9	1.8	early interglacial	peak	decreasing
c	1995	18	1.9	early interglacial	spans full cycle	increasing half of cycle
d	2145	5	1.0	deglacial onset	increasing	late peak
e	2475	5	1.0	late deglacial-early interglacial	peak	peak
f	2500	4	1.0	late deglacial-early interglacial	early peak	decreasing

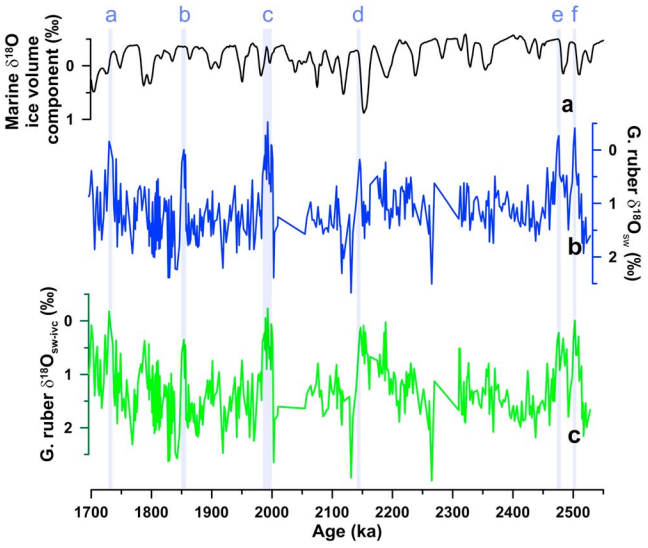

Figure 8. (c) 625 *G. ruber* $\delta^{18}O_{sw\text{-}ivc}$, derived by subtracting a reconstruction of (a) ocean $\delta^{18}O$ related to eustatic sea level changes [*Rohling et al.*, 2014] from the (b) 625 $\delta^{18}O_{sw}$ record.

events occurred during the late stages of deglaciations (as represented by the benthic $\delta^{18}O$ record) and often extended well into interglacial intervals (Figure 5f, 7e; Table 1). Two exceptions to this observation are event "a", which appears to occur in the middle of an interglacial and event "d", which falls near the onset of the benthic deglaciation.

To fully isolate the local seawater $\delta^{18}O$ signal related to meltwater, however, we must also consider changes in whole ocean $\delta^{18}O$ associated with ice volume variations. Only one continuous ice volume reconstruction independent of the marine $\delta^{18}O$ record exists for the early Pleistocene at present, which is based on hydraulic modeling of sea level-controlled exchange between the open ocean and Mediterranean Sea across the Strait of Gibraltar (Figure 8a) [*Rohling et al.*, 2014]. Subtracting this ocean $\delta^{18}O$ component from the 625 $\delta^{18}O_{sw}$ record has little effect on meltwater events "a", "b", and "c", but it pushes the onsets of events "d", "e", and "f" substantially earlier into the preceding glacial periods (Figure 7d). The robustness of this analysis, of course, rests on how well the 625 and Mediterranean records are lined up in time as well as the accuracy of the Mediterranean ocean $\delta^{18}O$ reconstruction; it will therefore be important to reconsider this ice volume correction as more early Pleistocene sea level reconstructions are developed. For now, we simply highlight the potential for ice volume effects to modify, though not remove, the 625 meltwater signals. In any case, this ice volume correction cannot account for the meltwater signals occurring or extending into interglacials in the benthic record.

This interglacial timing for LIS melt is difficult to reconcile with a simple interpretation of the marine $\delta^{18}O$ record as primarily a proxy for Northern Hemisphere ice volume – otherwise, one would expect meltwater events from the southern LIS, presumably the first region to deglaciate, to consistently line up with the first half of benthic terminations, much as observed for the most recent deglaciation (Figure 3f, 7e) [*Flower et al.*, 2004; *Schmidt and Lynch-Stieglitz*, 2011; *Wickert et al.*, 2013]. What might explain this perplexing relationship between LIS meltwater events and benthic $\delta^{18}O$? If deep ocean temperature led ice volume during the early Pleistocene, ice melt might have exhibited a late phasing relative to benthic $\delta^{18}O$. Indeed, several high latitude surface and deep ocean temperature reconstructions do suggest an early timing for ocean temperature changes on the order of millennia [*Bintanja and van de Wal*, 2008; *Dwyer et al.*, 1995; *Elderfield et al.*, 2012; *Lawrence et al.*, 2009; *Sosdian and Rosenthal*, 2009], though this might not be large enough to fully account for the late phase of some of the GOM meltwater events. Another possibility is that some LIS variability is masked in marine $\delta^{18}O$ by opposing ice volume changes elsewhere, such as over precession cycles in Antarctica as proposed by the Antiphase hypothesis [*Raymo et al.*, 2006]. This suggestion is bolstered by recent studies that have detected early Pleistocene precession variability in Southern Ocean ice-rafted debris [*Patterson et al.*, 2014] as well as in a sub-Antarctic SST record that is in phase with Southern Hemisphere insolation forcing prior to 1600 ka [*Martínez-Garcia et al.*, 2010].

To evaluate this possibility, we use the relationship between the meltwater events (as defined by $\delta^{18}O_{sw}$) and potential orbital forcings to test the predictions of the Integrated Insolation [*Huybers*, 2006] and Antiphase [*Raymo et al.*, 2006] hypotheses. One would expect the meltwater events to occur during the rising limb or perhaps near the peak of the relevant forcing, much as it does during the last deglaciation with boreal summer insolation (Figure 3e, 7a). This comparison does not reveal a decisive link to either hypothesis, but it does

suggest a closer association with summer insolation than obliquity – five meltwater events fall on the rising limb or peak of summer insolation forcing (b, c, d, e, and f), but only three events (a, c, and e) line up with rising or maximum obliquity while the other three (b, d, and f) occur during the falling half of the obliquity cycle (Figure 7, Table 1). Notably, the events most in sync with summer insolation are also the best dated – the benthic $\delta^{18}O$ chronology is clear for events "b", "d", "e", and "f", and the latter three events fall at or near the peak of SST precession cycles. We reiterate, however, that correcting the $\delta^{18}O_{sw}$ record for ice volume changes may alter the length and midpoint of some of the meltwater events (Figure 7d); therefore, the relationships to orbital forcing suggested here should be considered tentative.

6.2.2. Magnitude and Duration of Meltwater Events

The magnitude of the meltwater events ranges from 1–2 ‰ (Table 1), which tends to fall within the range of GOM meltwater events observed during MIS 3 (~1 ‰) and the last deglaciation (up to 3 ‰) in the Orca Basin (Figure 7c) [*Flower et al.*, 2004; *Hill et al.*, 2006; *Wickert et al.*, 2013]. This comparison is complicated, however, by potential differences in the location of the records relative to meltwater plumes (Figure 2), changes in the position of continental runoff or the Loop Current through time, signal smoothing associated with bioturbation, sample resolution, and the possibly differing isotopic composition of the LIS during the early and late Pleistocene. It is difficult to quantitatively assess most of these effects, though as a starting point for a more direct comparison, we resampled the last deglacial $\delta^{18}O_{sw\text{-}ivc}$ event in the Orca Basin at the 2-kyr resolution and 0.5-kyr smoothing (i.e., the amount of time averaged in our 2 cm-thick samples) of our early Pleistocene record. This resampling reduces the magnitude of the Orca Basin deglacial $\delta^{18}O_{sw\text{-}ivc}$ spike to ~2‰ – comparable to the early Pleistocene anomalies – and the event becomes composed of one, or at most two, datapoints (Figure 7d). Furthermore, the LIS may have been isotopically heavier during the early Pleistocene due to its possibly lower profile [*Bailey et al.*, 2010], which would also make the early Pleistocene meltwater events appear more muted relative to the last deglacial event than they actually are.

The duration of the early Pleistocene meltwater events also appear remarkable, insofar as the thickness of the signal in the sediments is an accurate proxy for time (i.e., sedimentation rates are constant). The GOM meltwater spike during the last deglaciation encompassed 4.5 kyr in total, and the main interval of elevated $\delta^{18}O_{sw}$ values lasted only 3 kyr (Figure 3c) [*Wickert et al.*, 2013]. Early Pleistocene events, in contrast, span 20–75 cm of sediment, or 4–18 kyr on our age model (Figure 7c, Table 1). In addition, correcting 625 $\delta^{18}O_{sw}$ for ice volume effects would further lengthen several of these events (Figure 7d). We cannot exclude the possibility that sedimentation rates temporarily increased in association with meltwater events, giving the false impression of lengthy event durations, but this would also lead to an obvious distortion in the benthic $\delta^{18}O$ record, which we do not see. Furthermore, sedimentation rates are not especially high during the last deglacial meltwater event in the well-dated Orca Basin record (Figure 3d) [*Williams et al.*, 2010]. Whereas bioturbation could also temporally stretch a meltwater signal, this effect typically occurs within the top 10 cm of the sediment column [*Teal et al.*, 2008], considerably thinner than the thicknesses of the 625 meltwater signals. Moreover, a number of the 625 events have abrupt onsets and terminations, rather than the smoother transitions that would be expected with vertical sediment mixing. In any case, bioturbation would increase the width of a meltwater signal at the expense of its amplitude [*Anderson*, 2001]; the area under $\delta^{18}O_{sw}$ anomaly curves may therefore provide a basis to compare the total meltwater flux associated with them (bearing the above caveats in mind).

Considering both event magnitude and duration together, we tentatively conclude that meltwater fluxes to the GOM during the early Pleistocene may have been comparable to or even larger than those in the late Pleistocene. This inference may suggest that the southern LIS was as large during the early Pleistocene as the late Pleistocene, despite the apparently smaller ice volume implied by the marine $\delta^{18}O$ record. The longer duration of early Pleistocene meltwater events relative to the late Pleistocene is also consistent with the more gradual terminations and greater symmetry of early Pleistocene glacial cycles inferred from benthic $\delta^{18}O$ [*Raymo*, 1992].

6.2.3. Frequency of Meltwater Events

The first meltwater event at ~2500 ka occurs shortly after the canonical intensification of Northern Hemisphere glaciation at ~2700 ka [*Raymo et al.*, 1989], confirming that the LIS was areally extensive near the beginning of the Pleistocene [*Joyce et al.*, 1990], and perhaps correlates with a Missouri till dated to 2421 ± 143 ka by $^{26}Al/^{10}Be$ burial dating (Figure 1c, 2) [*Balco and Rovey*, 2010]. While our multi-proxy record does not extend into the Pliocene, the *Joyce et al.* [1990, 1993] planktic $\delta^{18}O$ data show no earlier negative

isotope anomalies (Figure 1a), suggesting that this 2500 ka meltwater event is the first one. In contrast to the numerous meltwater events in our record, however, the mid-continent till record does not indicate another extensive ice advance until the mid-Pleistocene at 1300 ka (Figure 1c) [*Balco and Rovey*, 2010]. This lack of early Pleistocene tills for every meltwater event suggests that later advances eroded them away.

The GOM record clearly does not show meltwater events associated with every glacial cycle, however, which could be explained in two ways. This may reflect shifts in the location of meltwater plumes away from Site 625 at times, due to a migrating Mississippi delta or GOM surface currents. Indeed, 625 does not appear to record the last deglacial meltwater pulse [*Whitaker*, 2008; *Ziegler et al.*, 2008] seen elsewhere in the GOM (Figure 3) [*Kennett and Shackleton*, 1975; *Schmidt and Lynch-Stieglitz*, 2011; *Wickert et al.*, 2013]. Alternatively, the LIS may only have advanced far enough south to reach the Mississippi drainage occasionally during the early Pleistocene.

The occurrence of the meltwater events do not reveal a particularly strong association with the magnitude of sea level changes inferred from the Mediterranean record (Figure 8) [*Rohling et al.*, 2014]. Event "d" corresponds with the first deep glacial in the sea level record at 2150 ka, but there are two events (e and f) several hundred kyr earlier when sea level fluctuations were half as large, and three events later (a, b, and c) that are not associated with sea level events. This disconnect between southern LIS melt and global sea level changes may further point to non-uniform ice volume variability around the world during the early Pleistocene, or else misinterpretations or misalignments of the 625 and Mediterranean Sea records.

6.3. Implications for Early Pleistocene Hypotheses

Although few in number, the GOM meltwater events provide several remarkable observations that do not readily square with the standard interpretation of early Pleistocene marine $\delta^{18}O$ as primarily recording smaller Northern Hemisphere ice sheets responding to obliquity [*Huybers*, 2007; *Pisias and Moore*, 1981; *Ruddiman et al.*, 1989]. While mid-continent tills have long shown that the LIS reached the mid-latitudes at least once in the earliest Pleistocene [*Balco et al.*, 2005; *Boellstorff*, 1978; *Roy et al.*, 2004], our GOM record indicates that this occurred at least six times prior to 1700 ka. The mere presence of the LIS at these southerly latitudes is inconsistent with the Integrated Insolation hypothesis, which requires ice to have remained north of 60°N, where obliquity forcing dominates, to produce 41-kyr glacial cycles [*Huybers and Tziperman*, 2008]. The sensitivity of the early Pleistocene LIS to precession forcing is further suggested by the phasing of the meltwater events with respect to orbital variations, which exhibit a closer association with precession-and-obliquity-controlled summer insolation intensity than obliquity-dominated integrated summer insolation. The late timing of meltwater events relative to deglaciations in benthic $\delta^{18}O$ also implies that this record is not a simple proxy of Northern Hemisphere ice volume variations, dominated by the LIS. Lastly, the relatively large size of the meltwater events suggests that the LIS may have frequently been as large in the early Pleistocene as the late Pleistocene, again in apparent conflict with an interpretation of the marine $\delta^{18}O$ record as a de facto Northern Hemisphere ice volume proxy.

Rather, the meltwater events may be easier to reconcile with the Antiphase hypothesis. This model invokes large early Pleistocene ice sheets driven by summer insolation intensity, the expression of which are largely decoupled from the marine $\delta^{18}O$ record due to hemispheric cancellation of ice volume variability at precession time scales, which dramatically weakens precession power in $\delta^{18}O$ as well as the amplitude of the record [*Raymo et al.*, 2006].

The Antiphase view raises several questions concerning LIS dynamics and North Atlantic climate though, which we briefly mention and offer some thoughts on. First, how could the 23-kyr LIS variability predicted by the Antiphase hypothesis be reconciled with the strong 41-kyr signal present in numerous North Atlantic records? *Raymo et al.* [2006] suggest that ice-rafted debris delivery to the North Atlantic was controlled by the stability of LIS marine margins, driven in turn by global sea level changes that followed the hemispherically in-phase obliquity forcing. More difficult to explain is the dominant 41-kyr variability in North American biomarker dust fluxes to Site U1313 in the North Atlantic [*Naafs et al.*, 2012], originally interpreted to reflect dust generation by glacial grinding, but argued by *Lang et al.* [2014] to be sourced from the mid latitudes by non-glaciogenic processes. North American dust fluxes could be decoupled from summer insolation-driven LIS fluctuations if dust generation/mobilization was controlled by winter insolation, latitudinal insolation gradients, greenhouse gas forcing that may have had a 41-kyr rhythm [*Herbert et al.*, 2010], or sand-blasting of vegetation colonizing exposed continental shelves following sea level fall.

Second, if the LIS was larger than typically inferred from the marine $\delta^{18}O$ record during the early Pleistocene, why was this interval not characterized by pronounced millennial variability like the Hudson Strait-Heinrich and Dansgaard-Oeschger events of the late Pleistocene [*Hodell and Channell*, 2016]? Perhaps the LIS was lower slung and did not attain the thickness required to induce widespread basal melt and Heinrich-like purging [*MacAyeal*, 1993] or nonlinear interactions with the atmospheric flow and attendant climate switches [*X. Zhang et al.*, 2014]. It has also been suggested that Heinrich events are related to the duration of glacial periods [*Hodell et al.*, 2008], in which case early Pleistocene glaciations may have been too short to trigger them. A final possibility is that the early Pleistocene was too warm to allow buttressing ice shelves or extensive sea ice cover to develop in the North Atlantic and facilitate ice sheet and climate instability.

Third, if the LIS grew as large during the early Pleistocene as the late Pleistocene, how did this occur given that glacial cycles were apparently much shorter during the earlier interval? The Regolith Hypothesis suggests that the ice sheet may not necessarily have added volume any faster in the early Pleistocene, but it flowed faster over a deformable bed to more quickly attain a late Pleistocene-like extent. Alternatively, the reduction in millennial-scale climate variability during the early Pleistocene may have allowed the ice sheet to grow more quickly, uninterrupted by repeated melt events from interstadial warmings [*Hill et al.*, 2006]. It is also possible that the warmer, moister atmosphere of the early Pleistocene increased the snowfall rate on the ice sheet.

6.4. The Need for More Cores

For 25 years, 625 planktic $\delta^{18}O$ has provided a singularly valuable record of LIS melt spanning the Plio-Pleistocene [*Joyce et al.,* 1990, 1993] and has challenged the canonical view of early Pleistocene ice sheets as typically smaller than those observed during the late Pleistocene. Unbelievably, after a quarter of a century, there is still no other long marine record adjacent to any major drainage outlets of the LIS. The planktic data and benthic chronology added in this study confirm the meltwater events identified by Joyce et al. and suggest several curious aspects regarding their timing, size, and frequency, not all of which readily fit into standard interpretations of Pleistocene climate. Unfortunately, the 625 core is of extremely poor quality (by current standards) with likely missing sections at numerous core breaks resulting in the benthic $\delta^{18}O$ correlation to LR04 being ambiguous in places. Additionally, too few meltwater events are recorded to be statistically useful, and most importantly, this single site cannot resolve whether the lack of more meltwater events simply reflects Mississippi delta and meltwater plume migration away from the core site at times or a true absence of LIS advances into the mid-latitudes and meltwater fluxes to the GOM. Given the discontinuity of the geologic record on land, it seems likely that an array of cores from the GOM would ultimately be needed to firmly resolve the nature of southern LIS variability over the past few million years and the mechanisms that control ice sheet mass balance on orbital time scales.

7. Conclusions

An 850-kyr long early Pleistocene record of planktic $\delta^{18}O$, Mg/Ca SSTs, and benthic $\delta^{18}O$ from the northern GOM sheds light on climate and ice sheet dynamics in the 41-kyr world. SSTs tend to co-vary with glacial cycles recorded in benthic $\delta^{18}O$, but SSTs exhibit substantially more precession variability, much as they do during the late Pleistocene [*Ziegler et al.*, 2008]. SSTs exhibit greater glacial-interglacial variability over the Pleistocene, but show no long-term trend, which may be a pattern common to tropical warm pools or which might reflect proxy bias. Extracting the $\delta^{18}O_{sw}$ component of planktic $\delta^{18}O$ using the SST record shows six irregularly spaced negative isotope anomalies – at 1730, 1855, 1995, 2145, 2475, and 2500 ka – that likely record meltwater pulses associated with LIS advances into the Mississippi River basin. These meltwater events tend to occur during the late stages of benthic deglaciations and extend into interglaciations, which suggests that benthic $\delta^{18}O$ might not provide a simple proxy for Northern Hemisphere ice volume dominated by the LIS (e.g., [*Raymo et al.*, 2006]). The $\delta^{18}O_{sw}$ anomalies are similar in size to the GOM meltwater signal from the last deglaciation (after accounting for differences in sample resolution) and they appear longer in duration; it is therefore conceivable that southern LIS meltwater fluxes during the early Pleistocene were comparable to or larger than those observed during the late Pleistocene. Lastly, the timing of most of the meltwater events are consistent with forcing by the obliquity-and-precession-controlled

intensity of summer insolation, while fewer events line up with the obliquity-dominated integrated summer insolation forcing. Although few in number, these meltwater events seem to suggest that a large LIS advanced into the mid-latitudes numerous times during the early Pleistocene and was sensitive to precession forcing – findings difficult to reconcile with the classical view that early Pleistocene ice volume variability was dominated by small Northern Hemisphere ice sheets controlled by obliquity.

Acknowledgments
We gratefully acknowledge the contribution of Ben Costanza to the development of the benthic chronology at Site 625. We also thank Dorothy Pak, Georges Paradis, Katherine Esswein, Janet Fang, Mieke Thierens, June Padman, and Andy Ross for help with sample processing and measurement, Anders Carlson for helpful discussion, and acknowledge support from the NOAA Climate and Global Change Postdoctoral Fellowship program, Boston College start-up funds, NSF award AGS-0823251 and ATM-0823251 to MER, and NSF award OCE-1260696, IMéRA and Aix-Marseille Université to DWL. Comments from Ian Bailey and two anonymous reviewers strengthened this manuscript. All dated generated in this study are given in the supplement.

References

Abe-Ouchi, A., F. Saito, K. Kawamura, M. E. Raymo, J. I. Okuno, K. Takahashi, and H. Blatter (2013), Insolation-driven 100,000-year glacial cycles and hysteresis of ice-sheet volume, *Nature*, *500*(7461), 190–193.

Aharon, P. (2006), Entrainment of meltwaters in hyperpycnal flows during deglaciation superfloods in the Gulf of Mexico, *Earth Planet. Sci. Lett.*, *241*(1–2), 260–270.

Anand, P., H. Elderfield, and M. H. Conte (2003), Calibration of Mg/Ca thermometry in planktonic foraminifera from a sediment trap time series, *Paleoceanography*, *18*(2), 1050, doi:10.1029/2002PA000846.

Anderson, D. M. (2001), Attenuation of millennial-scale events by bioturbation in marine sediments, *Paleoceanography*, *16*(4), 352–357, doi:10.1029/2000PA000530.

Antonov, J. I., D. Seidov, T. P. Boyer, R. A. Locarnini, A. V. Mishonov, H. E. Garcia, O. K. Baranova, M. M. Zweng, and D. R. Johnson (2010), World Ocean Atlas 2009 Volume 2: Salinity, in *NOAA Atlas NESDIS 69*, edited by S. Levitus, 184 pp., U.S. Gov. Print. Off., Washington, D. C.

Arbuszewski, J., P. deMenocal, A. Kaplan, and E. C. Farmer (2010), On the fidelity of shell-derived $\delta^{18}O$seawater estimates, *Earth Planet. Sci. Lett.*, *300*(3–4), 185–196.

Bailey, I., C. T. Bolton, R. M. DeConto, D. Pollard, R. Schiebel, and P. A. Wilson (2010), A low threshold for North Atlantic ice rafting from "low-slung slippery" late Pliocene ice sheets, *Paleoceanography*, *25*, PA1212, doi:10.1029/2009PA001736.

Balco, G., and C. W. Rovey (2010), Absolute chronology for major Pleistocene advances of the Laurentide Ice Sheet, *Geology*, *38*(9), 795–798.

Balco, G., J. O. Stone, and C. Rovey (2005), The First Glacial Maximum in North America, *Science*, *307*, 222.

Barker, S., M. Greaves, and H. Elderfield (2003), A study of cleaning procedures used for foraminiferal Mg/Ca paleothermometry, *Geochem. Geophys. Geosyst.*, *4*(9), 8407, doi:10.1029/2003GC000559.

Bell, D. B., S. J. A. Jung, and D. Kroon (2015), The Plio-Pleistocene development of Atlantic deep-water circulation and its influence on climate trends, *Quat. Sci. Rev.*, *123*, 265–282.

Bemis, B. E., H. J. Spero, J. Bijma, and D. W. Lea (1998), Reevaluation of the oxygen isotopic composition of planktonic foraminifera: Experimental results and revised paleotemperature equations, *Paleoceanography*, *13*(2), 150–160, doi:10.1029/98PA00070.

Berger, A., X. S. Li, and M. F. Loutre (1999), Modelling northern hemisphere ice volume over the last 3 Ma, *Quat. Sci. Rev.*, *18*(1), 1–11.

Berggren, W., F. Hilgen, C. Langereis, D. Kent, J. Obradovich, I. Raffi, M. Raymo, and N. Shackleton (1995), Late Neogene chronology: New perspectives in high-resolution stratigraphy, *GSA Bull.*, *107*, 1272–1287.

Bintanja, R., and R. S. W. van de Wal (2008), North American ice-sheet dynamics and the onset of 100,000-year glacial cycles, *Nature*, *454*(7206), 869–872.

Boellstorff, J. (1978), Chronology of some late Cenozoic deposits from the central United States and the ice ages, *Trans. Nebr. Acad. Sci.*, *6*, 35–49.

Clark, P. U., and D. Pollard (1998), Origin of the middle Pleistocene transition by ice sheet erosion of regolith, *Paleoceanography*, *13*, 1–9, doi:10.1029/97PA02660.

Clement, B. (1985), ODP leg 100 preliminary report, *Rep.*, Ocean Drilling Program, Texas A&M Univ., College Station.

Costanza, B. (2007), Late Pliocene/early Pleistocene glacial meltwater discharge to the Gulf of Mexico: Evidence from ODP Site 625, Boston Univ.

Dekens, P. S., D. W. Lea, D. K. Pak, and H. J. Spero (2002), Core top calibration of Mg/Ca in tropical foraminifera: Refining paleotemperature estimation, *Geochem. Geophys. Geosyst.*, *3*(4), 1022, doi:10.1029/2001GC000200.

Dwyer, G. S., T. M. Cronin, P. A. Baker, M. E. Raymo, J. S. Buzas, and T. Corrège (1995), North Atlantic Deepwater Temperature Change During Late Pliocene and Late Quaternary Climatic Cycles, *Science*, *270*(5240), 1347–1351.

Elderfield, H., P. Ferretti, M. Greaves, S. Crowhurst, I. N. McCave, D. Hodell, and A. M. Piotrowski (2012), Evolution of Ocean Temperature and Ice Volume Through the Mid-Pleistocene Climate Transition, *Science*, *337*(6095), 704–709.

Evans, D., and W. Müller (2012), Deep time foraminifera Mg/Ca paleothermometry: Nonlinear correction for secular change in seawater Mg/Ca, *Paleoceanography*, *27*, PA4205, doi:10.1029/2012PA002315.

Fedorov, A. V., C. M. Brierley, K. T. Lawrence, Z. Liu, P. S. Dekens, and A. C. Ravelo (2013), Patterns and mechanisms of early Pliocene warmth, *Nature*, *496*(7443), 43–49.

Flower, B. P., D. W. Hastings, H. W. Hill, and T. M. Quinn (2004), Phasing of deglacial warming and Laurentide Ice Sheet meltwater in the Gulf of Mexico, *Geology*, *32*(7), 597–600.

Flowers, G. W., H. Björnsson, F. Palsson, and G. Clarke (2004), A coupled sheet-conduit mechanisms for jökulhlaup propagation, *Geophys. Res. Lett.*, *31*, L05401, doi:10.1029/2003GL019088.

Herbert, T. D., L. C. Peterson, K. T. Lawrence, and Z. Liu (2010), Tropical Ocean Temperatures Over the Past 3.5 Million Years, *Science*, *328*(5985), 1530–1534.

Hill, H. W., B. P. Flower, T. M. Quinn, D. J. Hollander, and T. P. Guilderson (2006), Laurentide Ice Sheet meltwater and abrupt climate change during the last glaciation, *Paleoceanography*, *21*, PA1006, doi:10.1029/2005PA001186.

Hodell, D. A., and J. E. T. Channell (2016), Mode transitions in Northern Hemisphere Glaciation: Co-evolution of millennial and orbital variability in Quaternary climate, *Clim. Past Discuss.*, *2016*, 1–55.

Hodell, D. A., J. E. T. Channell, J. H. Curtis, O. E. Romero, and U. Röhl (2008), Onset of "Hudson Strait" Heinrich events in the eastern North Atlantic at the end of the middle Pleistocene transition (~640 ka), *Paleoceanography*, *23*, PA4218, doi:10.1029/2008PA001591.

Hönisch, B., K. A. Allen, A. D. Russell, S. M. Eggins, J. Bijma, H. J. Spero, D. W. Lea, and J. Yu (2011), Planktic foraminifers as recorders of seawater Ba/Ca, *Mar. Micropaleontol.*, *79*(1–2), 52–57.

Huybers, P. (2006), Early Pleistocene glacial cycles and the integrated summer insolation forcing, *Science*, *313*(5786), 508–511.

Huybers, P. (2007), Glacial variability over the last two million years: An extended depth-derived agemodel, continuous obliquity pacing, and the Pleistocene progression, *Quat. Sci. Rev.*, *26*(1–2), 37–55.

Huybers, P. (2011), Combined obliquity and precession pacing of late Pleistocene deglaciations, *Nature*, *480*(7376), 229–232.

Huybers, P., and E. Tziperman (2008), Integrated summer insolation forcing and 40,000-year glacial cycles: The perspective from an ice-sheet/energy-balance model, *Paleoceanography*, *23*, PA1208, doi:10.1029/2007PA001463.
Imbrie, J., and J. Z. Imbrie (1980), Modeling the climatic response to orbital variations, *Science*, *207*, 943–953.
Joyce, J. E., L. R. C. Tjalsma, and J. M. Prutzman (1990), High-resolution planktic stable isotope record and spectral analysis for the last 5.35 M.Y.: Ocean Drilling Program Site 625 northeast Gulf of Mexico, *Paleoceanography*, *5*(4), 507–529, doi:10.1029/PA005i004p00507.
Joyce, J. E., L. R. C. Tjaisma, and J. M. Prutzman (1993), North American glacial meltwater history for the past 2.3 m.y.: Oxygen isotope evidence from the Gulf of Mexico, *Geology*, *21*(6), 483–486.
Kennett, J. P., and N. J. Shackleton (1975), Laurentide ice sheet meltwater recorded in Gulf of Mexico deep-sea cores, *Science*, *188*, 147–150.
Klinkhammer, G. P., B. A. Haley, A. C. Mix, H. M. Benway, and M. Cheseby (2004), Evaluation of automated flow-through time-resolved analysis of foraminifera for Mg/Ca paleothermometry, *Paleoceanography*, *19*, PA4030, doi:10.1029/2004PA001050.
Lalicata, J. J., and D. W. Lea (2011), Pleistocene carbonate dissolution fluctuations in the eastern equatorial Pacific on glacial timescales: Evidence from ODP Hole 1241, *Mar. Micropaleontol.*, *79*, 41–51.
Lang, D. C., et al. (2014), The transition on North America from the warm humid Pliocene to the glaciated Quaternary traced by eolian dust deposition at a benchmark North Atlantic Ocean drill site, *Quat. Sci. Rev.*, *93*, 125–141.
Laskar, J., P. Robutel, F. Joutel, M. Gastineau, A. C. M. Correia, and B. Levrard (2004), A long term numerical solution for the insolation quantities of the Earth, *Astron. Astrophys.*, *428*, 261–285.
Lawrence, K. T., T. D. Herbert, C. M. Brown, M. E. Raymo, and A. M. Haywood (2009), High-amplitude variations in North Atlantic sea surface temperature during the early Pliocene warm period, *Paleoceanography*, *24*, PA2218, doi:10.1029/2008PA001669.
Lea, D. W., D. K. Pak, and H. J. Spero (2000), Climate impact of late Quaternary equatorial Pacific sea surface temperature variations, *Science*, *289*, 1719–1724.
Lea, D. W., D. K. Pak, and G. Paradis (2005), Influence of volcanic shards on foraminiferal Mg/Ca in a core from the Galápagos region, *Geochem. Geophys. Geosyst.*, *6*, Q11P04, doi:10.1029/2005GC000970.
LeGrande, A. N., and G. A. Schmidt (2006), Global gridded data set of the oxygen isotopic composition in seawater, *Geophys. Res. Lett.*, *33*, L12604, doi:10.1029/2006GL026011.
Lisiecki, L. E., and M. E. Raymo (2005), A Pliocene-Pleistocene stack of 57 globally distributed benthic δ18O records, *Paleoceanography*, *20*, PA1003, doi:10.1029/2004PA001071.
MacAyeal, D. R. (1993), Binge/purge oscillations of the Laurentide Ice Sheet as a cause of the North Atlantic's Heinrich events, *Paleoceanography*, *8*, 775–784, doi:10.1029/93PA02200.
Martin, P. A., and D. W. Lea (2002), A simple evaluation of cleaning procedures on fossil benthic foraminiferal Mg/Ca, *Geochem. Geophys. Geosyst.*, *3*(10), 8401, doi:10.1029/2001GC000280.
Martinez-Boti, M. A., G. L. Foster, T. B. Chalk, E. J. Rohling, P. F. Sexton, D. J. Lunt, R. D. Pancost, M. P. S. Badger, and D. N. Schmidt (2015), Plio-Pleistocene climate sensitivity evaluated using high-resolution CO2 records, *Nature*, *518*(7537), 49–54.
Martínez-Garcia, A., A. Rosell-Melé, E. L. McClymont, R. Gersonde, and G. H. Haug (2010), Subpolar Link to the Emergence of the Modern Equatorial Pacific Cold Tongue, *Science*, *328*(5985), 1550–1553.
Medina-Elizalde, M., and D. W. Lea (2010), Late Pliocene equatorial Pacific, *Paleoceanography*, *25*, PA2208, doi:10.1029/2009PA001780.
Medina-Elizalde, M., D. W. Lea, and M. S. Fantle (2008), Implications of seawater Mg/Ca variability for Plio-Pleistocene tropical climate reconstruction, *Earth Planet. Sci. Lett.*, *269*(3–4), 585–595.
Naafs, B. D. A., J. Hefter, G. Acton, G. H. Haug, A. Martínez-Garcia, R. Pancost, and R. Stein (2012), Strengthening of North American dust sources during the late Pliocene (2.7 Ma), *Earth Planet. Sci. Lett.*, *317–318*, 8–19.
Nisancioglu, K. H. (2004), Modeling the impact of atmospheric moisture transport on global ice volume, Ph D. thesis, Massachusetts Institute of Technology, Cambridge.
O'Brien, C. L., G. L. Foster, M. A. Martinez-Boti, R. Abell, J. W. B. Rae, and R. D. Pancost (2014), High sea surface temperatures in tropical warm pools during the Pliocene, *Nat. Geosci.*, *7*(8), 606–611.
Patterson, M. O., R. McKay, T. Naish, C. Escutia, F. J. Jimenez-Espejo, M. E. Raymo, S. R. Meyers, L. Tauxe, H. Brinkhuis, and I. E. Scientists (2014), Orbital forcing of the East Antarctic ice sheet during the Pliocene and Early Pleistocene, *Nat. Geosci.*, *7*(11), 841–847.
Pisias, N. G., and T. C. Moore Jr. (1981), The evolution of Pleistocene climate: a time series approach, *Earth Planet. Sci. Lett.*, *52*, 450–458.
Raymo, M. E. (1992), Global Climate Change: A Three Million Year Perspective, in *Start of a Glacial*, edited by G. J. Kukla and E. Went, pp. 207–223, Springer, Berlin.
Raymo, M. E. (1997), The timing of major climate terminations, *Paleoceanography*, *12*(4), 577–585, doi:10.1029/97PA01169.
Raymo, M. E., and K. H. Nisancioglu (2003), The 41 kyr world: Milankovitch's other unsolved mystery, *Paleoceanography*, *18*(1), 1011, doi:10.1029/2002PA000791.
Raymo, M. E., W. F. Ruddiman, J. Backman, B. M. Clement, and D. G. Martinson (1989), Late Pliocene variations in northern hemisphere ice sheets and North Atlantic deep water circulation, *Paleoceanography*, *4*, 413–446, doi:10.1029/PA004i004p00413.
Raymo, M. E., L. E. Lisiecki, and K. H. Nisancioglu (2006), Plio-Pleistocene ice volume, Antarctic climate, and the global d18O record, *Science*, *313*, 492–495.
Rohling, E. J., G. L. Foster, K. M. Grant, G. Marino, A. P. Roberts, M. E. Tamisiea, and F. Williams (2014), Sea-level and deep-sea-temperature variability over the past 5.3 million years, *Nature*, *508*(7497), 477–482.
Roy, M., P. U. Clark, R. W. Barendregt, J. R. Glasmann, and R. J. Enkin (2004), Glacial stratigraphy and paleomagnetism of late Cenozoic deposits of the north-central United States, *Geol. Soc. Am. Bull.*, *116*(1–2), 30–41.
Ruddiman, W. F., M. E. Raymo, D. G. Martinson, B. M. Clement, and J. Backman (1989), Pleistocene evolution: Northern hemisphere ice sheets and North Atlantic ocean, *Paleoceanography*, *4*, 353–412, doi:10.1029/PA004i004p00353.
Schmidt, M. W., and J. Lynch-Stieglitz (2011), Florida Straits deglacial temperature and salinity change: Implications for tropical hydrologic cycle variability during the Younger Dryas, *Paleoceanography*, *26*, PA4205, doi:10.1029/2011PA002157.
Sosdian, S., and Y. Rosenthal (2009), Deep-Sea Temperature and Ice Volume Changes Across the Pliocene-Pleistocene Climate Transitions, *Science*, *325*(5938), 306–310.
Teal, L. R., M. T. Bulling, E. R. Parker, and M. Solan (2008), Global patterns of bioturbation intensity and mixed depth of marine soft sediments, *Aquat. Biol.*, *2*, 207–218.
Wagner, A. J., and N. C. Slowey (2011), Oxygen isotopes in seawater from the Texas-Louisiana shelf, *Bull. Mar. Sci.*, *87*, 1–12.
Weaver, P., and M. Raymo (1989), *Late Miocene to Holocene Planktonic Foraminifers from the Equatorial Atlantic, Leg 108*, edited by W. Ruddiman et al., pp. 71–91, Texas A&M Univ., College Station.
Whitaker, J. L. (2008), Orbital- to millennial-scale variability in Gulf of Mexico sea surface temperature and salinity during the late Pleistocene, M.S. thesis, Univ. of South Florida.

Wickert, A. D., J. X. Mitrovica, C. Williams, and R. S. Anderson (2013), Gradual demise of a thin southern Laurentide ice sheet recorded by Mississippi drainage, *Nature*, *502*(7473), 668–671.
Williams, C., B. P. Flower, D. W. Hastings, T. P. Guilderson, K. A. Quinn, and E. A. Goddard (2010), Deglacial abrupt climate change in the Atlantic Warm Pool: A Gulf of Mexico perspective, *Paleoceanography*, *25*, PA4221, doi:10.1029/2010PA001928.
Zhang, X., G. Lohmann, G. Knorr, and C. Purcell (2014), Abrupt glacial climate shifts controlled by ice sheet changes, *Nature*, *512*(7514), 290–294.
Zhang, Y. G., M. Pagani, and Z. Liu (2014), A 12-Million-Year Temperature History of the Tropical Pacific Ocean, *Science*, *344*(6179), 84–87.
Ziegler, M., D. Nurnberg, C. Karas, R. Tiedemann, and L. J. Lourens (2008), Persistent summer expansion of the Atlantic Warm Pool during glacial abrupt cold events, *Nat. Geosci.*, *1*(9), 601–605.